Rabeprazole attenuates fibrosis by modulating SMAD3 linker region phosphorylation

LINKAI LI[1*], ZHEN LIANG[1*], LONG FAN[1], YAJUN CAO[1], XIUFU TANG[2] and JIHUI CHEN[1]

[1]Department of Pharmacy, Zhuhai Center for Maternal and Child Health Care, Zhuhai, Guangdong 519000, P.R. China;
[2]Department of Pediatric Hematology and Rheumatology, Zhuhai Women and Children's Hospital, Zhuhai, Guangdong 519001, P.R. China

Received April 30, 2025; Accepted November 7, 2025

DOI: 10.3892/br.2025.2098

Abstract. Epithelial-to-mesenchymal transition (EMT) and fibrosis are well-established biological outcomes of TGFβ-mediated signaling. Rabeprazole, a proton pump inhibitor (PPI), has been widely used as a first-line therapy for *H. pylori* infection. However, the possible role of rabeprazole in fibrosis remains unclear. Western blotting and reverse transcription-quantitative PCR were used to analyze gene expression at mRNA and protein levels. In addition, immunofluorescence, immunoprecipitation (IP) and dual luciferase reporter assays were performed to identify the mechanism underlying rabeprazole-modulated fibrosis. Plasmid transfection was conducted to rescue the experiments. In the present study, EMT inhibition was observed in gastric epithelial cells, including AGS and GES-1 cells, in response to rabeprazole treatment. Specifically, stimulation with rabeprazole 100 μM caused an upregulation of transcriptional intermediary factor 1γ (TIF1γ) expression, leading to a decrease in fibronectin (FN) and collagen type I alpha 1 chain (Col1a1) expression, whereas no significant variation was observed in the expression of α-smooth muscle actin expression. Moreover, depletion of TIF1γ expression largely blocked the influence of rabeprazole on Col1a1 and FN expression. Mechanistically, the IP analysis showed that endogenous SMAD family member 3 (SMAD3) interacted with TIF1γ, and this interaction was enhanced in response to rabeprazole, which further inhibited SMAD3 linker phosphorylation and nuclear translocation as evidenced through subcellular fractionation experiments. Overall, the present findings reveal a previously unrecognized antifibrotic activity of rabeprazole. These findings enriched the biological function of rabeprazole and highlight a novel regulatory mechanism underlying its antifibrotic activity.

Correspondence to: Dr Jihui Chen, Department of Pharmacy, Zhuhai Center for Maternal and Child Health Care, 543 Ningxi Road, Zhuhai, Guangdong 519000, P.R. China
E-mail: 389924285@qq.com

*Contributed equally

Key words: fibrosis, SMAD family member 3, linker phosphorylation, transcriptional intermediary factor 1γ

Introduction

Epithelial-to-mesenchymal transition (EMT) is a critical pathological feature in fibrosis-related diseases, including intestinal fibrosis and pulmonary fibrosis (1), and represents a highly dynamic, multi-stage process regulated by multiple signaling pathways that promote acquisition of the mesenchymal phenotype. In detail, external stimulation of signaling pathways, including TGFβ/Wnt, triggers a transcriptional program during EMT that induces the expression of the E-cadherin transcriptional repressor SNAIL, which promotes cell migration, invasiveness and fibrosis. The core process of EMT is characterized by epithelial cells losing polarity and intercellular connections to acquire a mesenchymal phenotype with enhanced mesenchymal traits such as collagen, fibronectin (FN), vimentin and α-smooth muscle actin (α-SMA) expression, as well as reduced epithelial adhesion protein E-cadherin expression (2-4). Proton pump inhibitors (PPIs) have been shown to have anticancer activity against several types of cancer. For instance, omeprazole destroyed cyclic AMP response element-binding protein (CREB)-binding protein (CBP)/p300-mediated SNAIL protein acetylation to induce its degradation, leading to the inhibition of EMT in cancer cells (5), while pantoprazole was shown to inactivate the Wnt/β-catenin signaling pathway to block the EMT process (6-8). Moreover, rabeprazole was shown to reduce resistance to temozolomide in glioma via EMT inhibition (9). Despite the fact that previous studies showed that PPIs can inhibit EMT, to date, there is no direct evidence fully describing the role of rabeprazole in fibrosis.

It is well known that SMAD family member 3 (SMAD3) is an important mediator of TGFβ-induced fibrosis or EMT, which can crosstalk with other pathways to modulate pathological progression. For example, Y-box binding protein 1, a member of the DNA/RNA-binding protein family, was reported to upregulate SMAD7 transcription or interact with SMAD3 to overcome the effect of TGFβ stimulation (10,11). In addition, transcriptional intermediary factor 1γ (TIF1γ; also known as TRIM33), a direct target of CREB, interacted with SMAD3 to antagonize SMAD3-induced fibrosis (12), which was in line with studies reporting on the anti-EMT function of

TIF1γ (13,14). Notably, the phosphorylation of SMAD3 linker (at the ser204, ser208, ser213 and Thr179 residues) was reported to accelerate nuclear shuttle of cytoplasmic SMAD3, which decreased the accessibility of non-phosphorylated SMAD3 to membrane-anchored TGFβ receptor type I (TGFβRI), leading to inhibition of SMAD3C phosphorylation (15,16). Moreover, TIF1γ has been shown to act as a SMAD4 ubiquitin ligase, either dissociating SMAD2/SMAD3-SMAD4 complexes or mediating polyubiquitylation and degradation of SMAD4, thereby promoting competitive binding of SMAD2/3 through the MH2 domain (17). In addition, TIF1γ was reported to occupy SMAD-binding elements to prevent SMAD2/3-mediated DNA binding (12). Based on these findings, it is hypothesized that this TIF1γ/SMAD3 complex may have an inhibitory effect on SMAD3 phosphorylation and nuclear translocation to ablate SMAD3-mediated gene transcription. However, the critical phosphorylation site of SMAD3 in response to the TIF1γ/SMAD3 complex remain unclear.

Rabeprazole, a classical PPI, was previously recognized to be involved in the modulation of inflammation (18,19), barrier function (20,21) and metabolism (22). The aim of the present study was to identify the novel biological function of rabepraozole in fibrosis and reveal the possible relationship between TIF1γ and SMAD3 through immunofluorescence (IF), immunoprecipitation (IP) and luciferase assays. providing significant implications for understanding the function of rabeprazole.

Materials and methods

Chemical reagents. Gibco™ BASIC DMEM (cat. no. C11995500BT) and fetal bovine serum (FBS) (Premium Plus; cat. no. A5669701) were purchased from Thermo Fisher Scientific, Inc. Rabeprazole (cat. no. HY-B0656) was purchased from MedChemExpress. Lipo8000™ transfection reagent (cat. no. C0533), nuclear and cytoplasmic protein extraction kit (cat. no. P0028) and cell lysis buffer for western blotting and immunoprecipitation (IP; cat. no. P0013) were purchased from Beyotime Institute of Biotechnology. shRNA-TIF1γ plasmids and TIF1γ promoter plasmid, were constructed and obtained from Youbio Biotech Co., Ltd. Protein A/G magnetic beads (cat. no. B23202) were purchased from Selleck Chemicals. EZ-press RNA Purification Kit (cat. no. B0004D), 4X EZscript Reverse Transcription Mix II (with gDNA Remover; cat. no. EZB-RT2G) and 2X Color SYBR Green qPCR Master Mix (cat. no. A0012) were purchased from EZBioscience. A dual-luciferase reporter assay system (cat. no. E1910) was obtained from Promega Corporation. Antibodies including α-SMA specific monoclonal antibody (mAb) (cat. no. 67735-1-Ig), FN mAb (cat. no. 66042-1-Ig), vimentin polyclonal antibody (pAb) (cat. no. 10366-1-AP), collagen type I (Col1a1) mAb (cat. no. 67288-1-Ig), SMAD3 mAb (cat. no. 66516-1-Ig), lamin A/C pAb (cat. no. 10298-1-AP) and α-tubulin mAb (cat. no. 66031-1-Ig) were purchased from Proteintech Group, Inc. TIF1γ mouse mAb (cat. no. YM1108), SMAD3 (phospho Ser204) rabbit pAb (cat. no. YP0363), SMAD3 (phospho Ser213) rabbit pAb (cat. no. YP0364), SMAD3 (phospho Thr179) rabbit pAb (cat. no. YP0745) and SMAD3 (phospho Ser208) rabbit pAb (cat. no. YP0746) were purchased from Immunoway Biotechnology Co., Ltd.; peroxidase affiniPure™ goat anti-rabbit IgG (H+L) (cat. no. 111-035-003) and peroxidase-conjugated affiniPure goat anti-mouse IgG (H+L) (cat. no. 115-035-003) were obtained from Jackson ImmunoResearch Laboratories, Inc.

Cell culture, treatment and transfection. Gastric epithelial cells, including AGS (cat. no. JNO-H0238) and GES-1 (cat. no. JNO-H0240), were purchased from Guangzhou Jennio Biotech Co. Ltd. and maintained in DMEM medium containing 10% FBS, 100 mg/ml streptomycin and 100 U/ml penicillin. Rabeprazole was dissolved in DMSO and stored at -80˚C. The concentration of rabeprazole used was 100 μM. For cell transfection of each well in a 6-well plate, when cells reached 50% confluence, 2 μg plasmids were gently mixed with 4 μl Lipo8000 transfection reagent in 125 μl Opti-MEM® medium at room temperature according to the manufacturer's instructions. Subseqently, the mix was added into each well for 48 h. pLVX-shRNA-PURO plasmids (cat. no. L28550-L28552) targeting TIF1γ (also known as TRIM33) were constructed and purchased from Youbio Biotech Co., Ltd.

Reverse transcription-quantitative (RT-q)PCR analysis. Following treatment, total RNA was extracted from 10^6 cells per group with the EZ-press RNA purification kit according to the manufacturer's instructions. cDNA was synthesized using 4X EZscript reverse transcription mix II (with gDNA Remover) to analyze the indicated gene expression using the 2X color SYBR Green qPCR Master Mix. The following primer pairs were used for qPCR: FN forward, 5'-TCAGCTTCCTGGCAC TTCTG-3' and reverse, 5'-TCTTGTCCTACATTCGGCGG-3'; vimentin forward, 5'-GGACCAGCTAACCAACGACA-3' and reverse, 5'-AAGGTCAAGACGTGCCAGAG-3'; COl1a1 forward, 5'-TCGGAGGAGAGTCAGGAAGG-3' and reverse, 5'-CCCGGTGACACATCAAGACA-3'; α-SMA forward, 5'-CTATGAGGGCTATGCCTTGCC-3' and reverse, 5'-GCT CAGCAGTAGTAACGAAGGA-3'; TIF1γ forward, 5'-AGC ACTACTATACAGCAAGCGA-3' and reverse, 5'-CAGAAG GTGGGATCACAATGG-3'; β-actin forward, 5'-CTTCGC GGGCGACGAT-3' and reverse, 5'-CCACATAGGAATCCT TCTGACC-3'.

Immunoblotting analysis. As described in Niu *et al* (23), after treatment, cells were harvested to extract the total protein using cell lysis buffer for western blotting and IP. Briefly, 15 μg total protein was separated by 10% SDS-PAGE and transferred into polyvinylidene fluoride (PVDF) membranes. The protein bands were blocked with PBST (0.5% Tween-20) (cat. no. BL345A) containing 2% skim milk (cat. no. BS102) plus 3% BSA (cat. no. BS114; all from Biosharp) for 1 h at room temperature. After washing with PBST (0.5% Tween-20), the membranes were incubated with the primary antibodies with a dilution of 1:2,000 overnight at 4˚C. Following incubation with primary antibodies, the membranes were incubated with the secondary antibodies at 1:2,000 for 1 h at room temperature. Finally, after washing with PBST, the bands were visualized and captured using Chemiluminescence imaging instrument (MiniChemi 610, Sinsage) after incubation with an ECL chemiluminescent substrate (cat. no. NEL105001EA; Revvity, Inc.). the density was quantified by Image J software (version: 1.8.0_351; National Institutes of Health) and normalized to internal control.

Subcellular isolation. According to the manufacturer's instructions, after serum starvation and when the cells reached 80% confluence, cells were treated with or without rabeprazole for 1 h at 37˚C and the cytosolic and nuclear fractions were extracted using the nuclear and cytoplasmic protein extraction kit aforementioned. Western blotting was performed to analyze the protein expression.

IP. As described in Li *et al* (24), when cells reached 80% confluence in a 6-cm dish, the medium was replaced with serum-free DMEM for 18 h. The cells were incubated with or without rabeprazole for 1 h, after which the medium was removed and the cells were washed with ice-cold PBS. The cells were then incubated with cell lysis buffer for western blotting and immunoprecipitation for 10 min on ice, scraped, and transferred into 1.5-ml tubes for an additional 30 min of lysis on a rotator at 4˚C. The lysates were centrifuged at 12,000 x g for 2 min at 4˚C to collect the supernatant. A total of 10 μl of anti-SMAD3 antibody was added to the supernatant and incubated overnight at 4˚C. Subsequently, 20 μl of protein A/G magnetic beads (cat. no. B23202; Selleck Chemicals) were added and incubated for 1 h at 4˚C to pull down the immune complexes. After three washes with cell lysis buffer for western blotting and IP (cat. no. P0013), the complexes were eluted with SDS loading buffer and boiled at 100˚C for 10 min for immunoblotting analysis.

Immunofluorescence staining. Cells were digested and reseeded into an 8-well slide overnight and incubated at 37˚C with or without rabeprazole for 1 h. After fixation with 3% PFA (cat. no. BL3786A) for 10 min at room temperature and permeabilization with 0.3% Triton X-100 (cat. no. BL935B; both from Biosharp; Beijing Labgic Technology Co., Ltd.) for 5 min at 4˚C, cells were blocked with 3% milk at room temperature for 1 h. The incubation with anti-SMAD3 at a dilution of 1:400 was conducted overnight at 4˚C. Subsequently, further incubation was performed for another 1 h at room temperature with goat anti-mouse IgG (H+L) (AbFluor 594) (cat. no. RS3608; Immunoway Biotechnology Co., Ltd.) at a dilution of 1:300. After washing and staining the nuclei with DAPI buffer (cat. no. C1006; Beyotime Insitute of Biotechnology) for 5 min at room temperature, the coverslips were covered with glass slides. Stained cells were visualized using a laser scanning fluorescent microscope (Leica Microsystems GmbH).

Dual luciferase reporter analysis. Briefly, the reporter plasmid containing 0.5 μg TIF1γ promoter in PGL3-Basic (cat. no. 56089) and 10 ng pRL-TK *Renilla* luciferase plasmid (cat. no. V1079; both from Youbio Biotech Co., Ltd.) at a ratio of 50:1 were co-transfected into cells in a 24-well plate at room temperature. Cells were maintained for 24 h with complete medium in a cell incubator using Lipo8000 transfection reagent (C0533; Beyotime Institute of Biotechnology), followed by incubation with 100 μM rabeprazole for another 24 h in serum-free medium at 37˚C. An equal precentage of DMSO was used as the vehicle control. Each group consisted of three replicates. The cells were lysed with 100 μl Passive Lysis Buffer, and samples were collected and measured using a plate-reading luminometer to calculate relative light units determined by the ratio of firely/*Renilla* to reflect TIF1γ transactivation, using the dual-luciferase reporter assay system (cat. no. E1910; Promega Corporation) according to the manufacturer's instructions.

Statistical analysis. Data analysis was performed with GraphPad Prism 10.0 (Dotmatics). Statistical comparisons between two groups were performed using the unpaired Student's t-test. One-sample t-test was conducted to analyze the RT-q PCR results. Statistical comparisons among three groups were performed using one-way ANOVA followed by the Dunnett's post hoc test. $P<0.05$ was considered to indicate a statistically significant difference.

Results

Rabeprazole suppresses fibrosis in gastric epithelial cells. AGS and GES-1 gastric epithelial cells were employed as *in vitro* models to assess the impact of rabeprazole on fibrotic processes. The expression levels of genes involved in fibrosis were analyzed in gastric epithelial cells after incubation for 24 h with rabeprazole at 10 and 100 μM. Compared with the control group (Fig. 1A and B), a significant fibrosis inhibition was observed in GES-1 and AGS cells in response to 100 μM rabeprazole stimulation as indicated by the largely decreased FN and Col1a1 mRNA levels, whereas no significant change was observed in vimentin mRNA expression regardless of treatment with 10 and 100 μM. Moreover, western blotting was performed to detect the indicated protein expression levels, and quantification of the indicated proteins revealed that rabeprazole treatment at 100 μM induced a downregulation of FN and Col1a1 expression in GES-1 and AGS cells, respectively, while no influence on vimentin expression was observed with treatment at 10 μM. In addition, the expression of α-SMA was downregulated in GES-1 cells (Fig. 1C and D). Taken together, these findings indicated that rabeprazole has a potent suppressive effect in inhibiting fibrosis.

TIF1γ is essential for the EMT inhibition mediated by rabeprazole. Since TIF1γ was reported to suppress extracellular matrix (ECM) production by inhibiting TGF-β1 transcriptional response (25-27), the present study focused on investigating the possible effect of rabeprazole on TIF1γ expression in gastric epithelial cells. Based on the previous results, treatment with 100 μM rabeprazole was selected for further experiments. Compared with the control group (Fig. 2A and B), the mRNA levels of TIF1γ were significantly increased in AGS and GES-1 cells in response to rabeprazole treatment. In addition, the protein expression level of TIF1γ was significantly enhanced by rabeprazole treatment (Fig. 2C). Moreover, dual luciferase reporter experiments further revealed that TIF1γ transactivation was significantly increased in response to rabeprazole treatment (Fig. 2D). Most importantly, depletion of TIF1γ expression by shRNA plasmid-targeted TIF1γ could rescue the effect of rabeprazole on FN and Col1a1 protein expression (Fig. 2E). These results indicated that rabeprazole inhibited the ECM through upregulation of TIF1γ expression.

Rabeprazole inhibits SMAD3 phosphorylation and nuclear translocation. It is well known that SMAD3 phosphorylation, whether in the linker domain or at the C-terminus, promotes

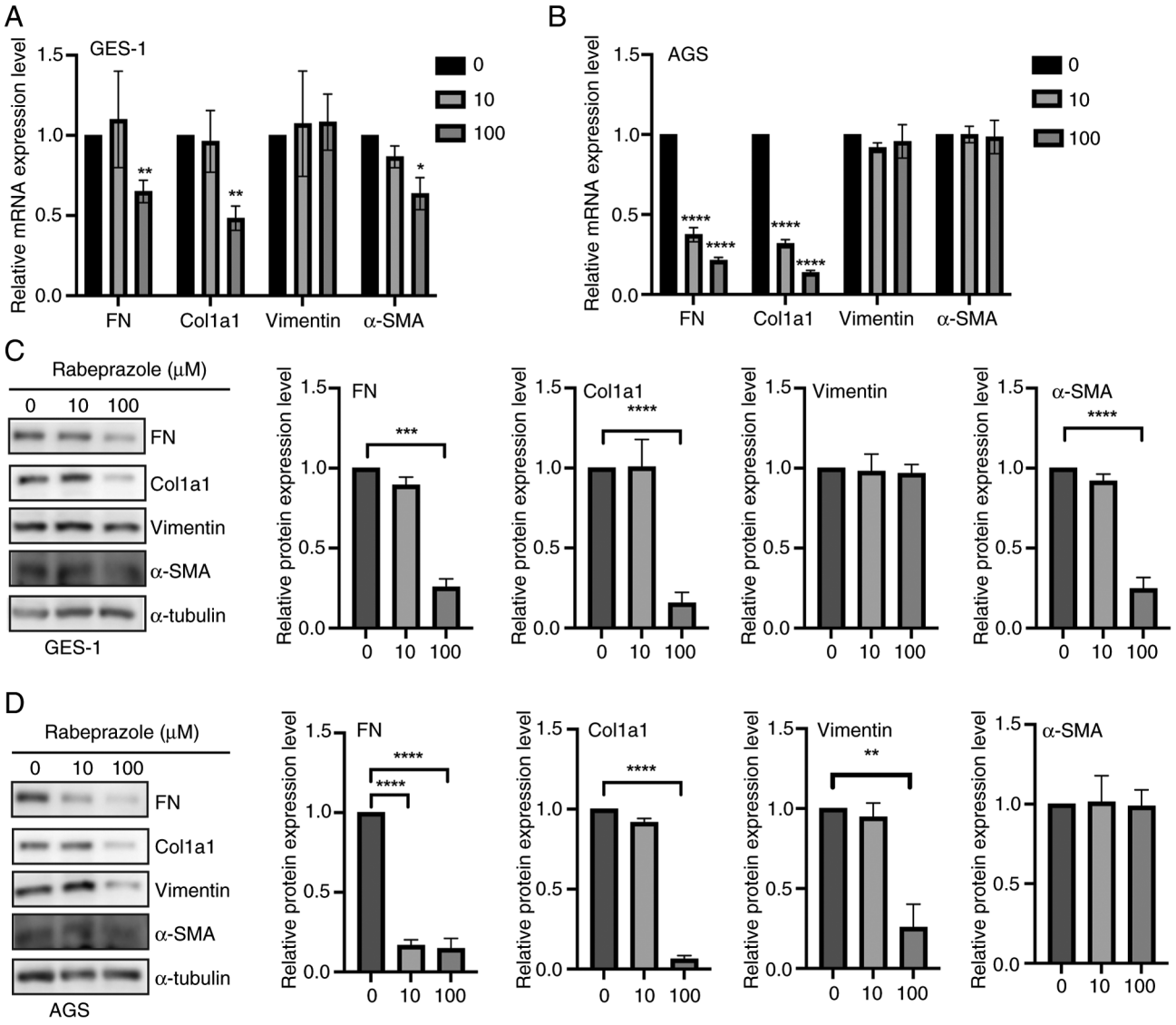

Figure 1. Rabeprazole inhibits fibrosis. After treatment with or without rabeprazole stimulation for 24 h at indicated concertations in (A) GES-1 and (B) AGS-1 cells, reverse transcription-quantitative PCR was conducted to analyze gene expression. Data was displayed as the mean ± SD and quantified by one-way ANOVA, followed by the Dunnett's post hoc test for significance against 0 μM. *P<0.05, **P<0.01 and ****P<0.0001; n=3. (C) GES-1 and (D) AGS cells were treated as previosuly described in (A and B). The total cells were harvested to detect the indicated protein levels. The quantitation of bands was analyzed using one-way ANOVA, followed by the Dunnett's post hoc test for significance against 0 μM. **P<0.01, ***P<0.001 and ****P<0.0001; n=3. FN, fibronectin; Col1a1, collagen type I alpha 1 chain; α-SMA, α-smooth muscle actin.

SMAD3 nuclear translocation to initiate gene transcription (16). Notably, a reciprocal inhibition existed between phosphorylation of the SMAD3 linker domain and C-terminus, which was attributed to the fact that SMAD3 phosphorylation at the linker domain could induce SMAD3 nuclear shuttling, thereby inhibiting the accessibility of non-phosphorylated SMAD3 to membrane-anchored TGFβRI (28).

The present results demonstrated that rabeprazole attenuated fibrosis, prompting an exploration of the influence of rabeprazole on SMAD3 activation. Through immunoblotting quantification, it was found that, in gastric epithelial cells, rabeprazole treatment led to a downregulation of SMAD3 phosphorylation at Ser204, Ser208 and Ser213, while no significant changes were observed at Thr179 of the SMAD3 linker domain (Fig. 3A-E). Moreover, subcellular fraction combined with immunofluorescence analysis further showed that the nuclear SMAD3 level was reduced in response to rabeprazole (Fig. 3F). Overall, rabeprazole inhibited SMAD3 phosphorylation and nuclear translocation.

Rabeprazole disrupts the interaction between SMAD3 and TIF1γ. The present study aimed to elucidate the mechanism by which rabeprazole influences fibrotic processes. SMAD3 was identified as a key transcriptional regulator of Col1a1, contributing to fibrosis via TGFβ-dependent signaling pathways (29). Notably, TIF1γ was shown to mitigate ECM accumulation by interacting with SMAD3, thereby attenuating fibrotic responses (12). These findings suggest that SMAD3 may play a pivotal role in the antifibrotic effects mediated by rabeprazole-induced TIF1γ activity. On this basis, the present study aimed to explore the possible relationship between SMAD3 and TIF1γ. As shown in Fig. 4A, endogenous SMAD3 interacted with TIF1γ, and this interaction was enhanced in response to rabeprazole. In line with this, immunoprecipitation

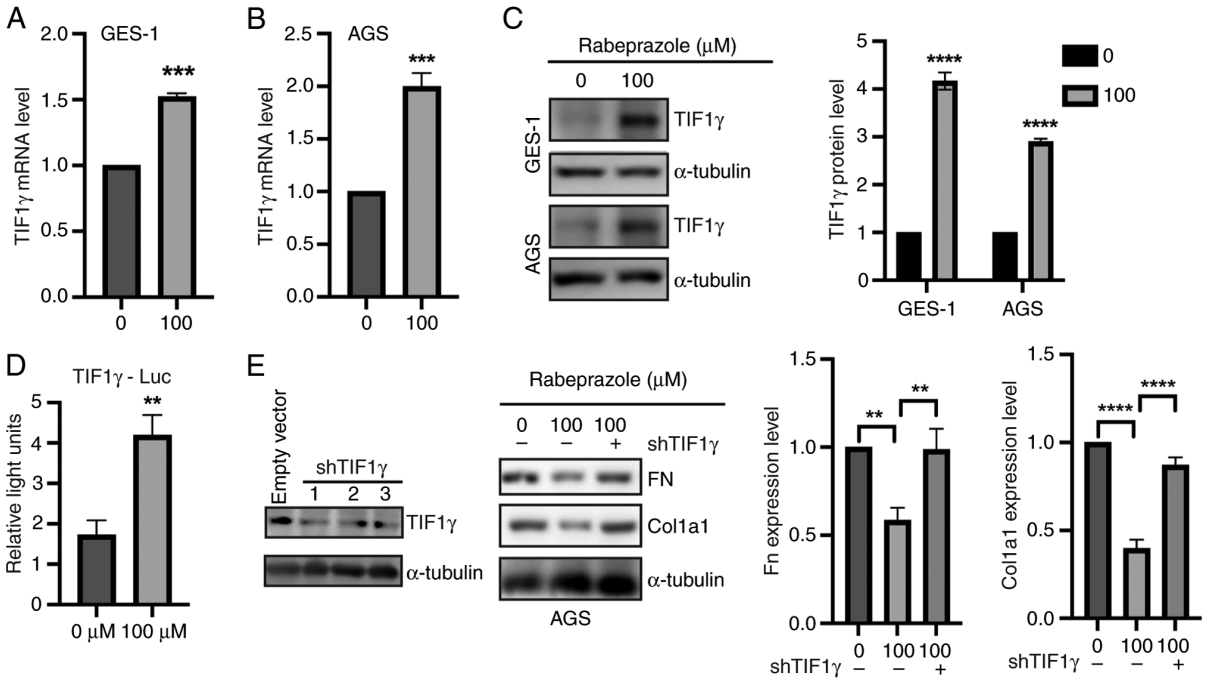

Figure 2. TIF1γ is essential for rabeprazole-modulated ECM. (A) GES-1 and (B) AGS cells were treated with or without rabeprazole for 48 h, and the expression of TIF1γ mRNA was analyzed by reverse transcription-quantitative PCR. Data are shown as the mean ± SD and quantified by one sample t-test for significance against 0 μM. ***P<0.001; n=3. (C) Western blotting was used to detect the protein level of TIF1γ in AGS cells in the absence or presence of rabeprazole for 48 h, and the bands were quantified and analyzed using one sample t-test. Data are displayed as the mean ± SD. ****P<0.0001; n=3. (D) TIF1γ promoter plasmid combined with *Renilla* plasmid were co-transfected into AGS cell for 24 h, followed by treatment with or without rabeprazole for another 24 h. Relative light units were measured using the dual-luciferase reporter assay system according to the manufacturer's instructions. Data are displayed as the mean ± SD and quantified by two sample t-test for significance against 0 μM. **P<0.01; n=3. (E) Following transfection with pooled shTIF1γ plasmids overnight, AGS cells were treated with or without rabeprazole for another 48 h, and the bands were quantified and analyzed using one sample t-test. **P<0.01 and ****P<0.0001; n=3. TIF1γ, transcriptional intermediary factor 1γ; FN, fibronectin; Col1a1, collagen type I alpha 1 chain.

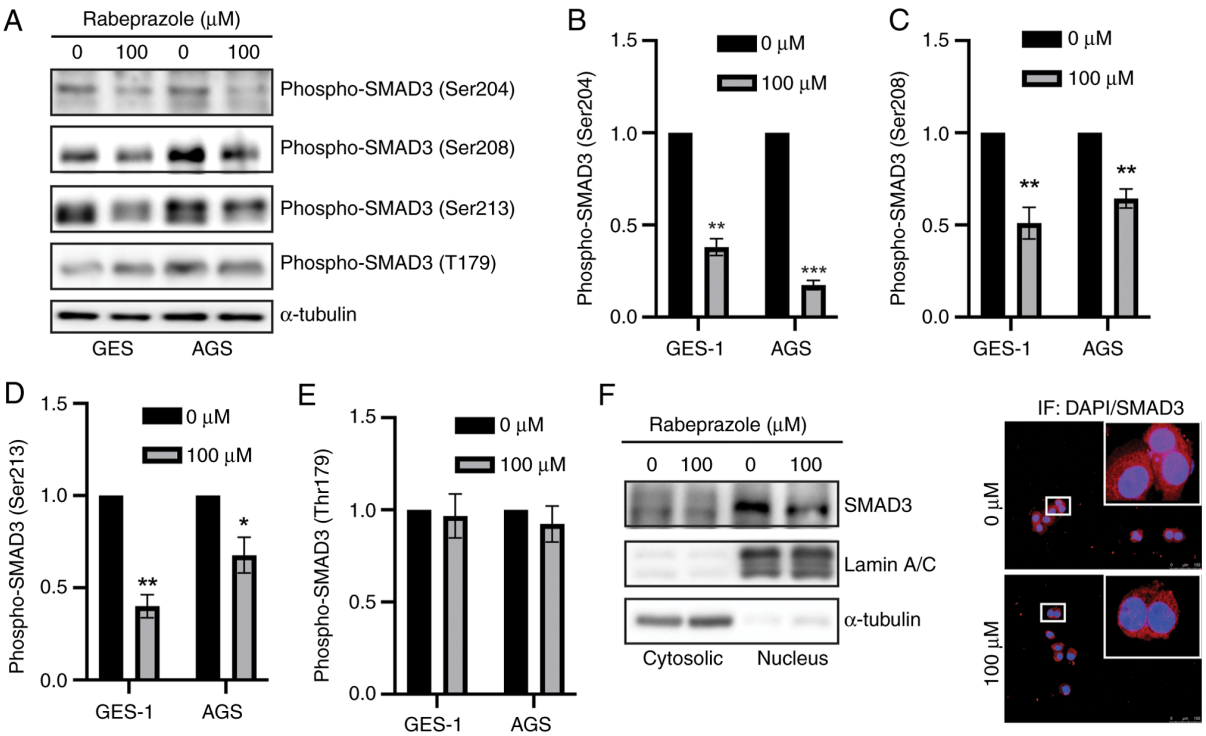

Figure 3. Rabeprazole modulates SMAD3 phosphorylation and nuclear translocation. (A) GES-1 and AGS cells were treated with or without rabeprazole for 1 h, and the phosphorylation of SMAD3 linker was detected by immunoblotting. (B-E) The band intensities were quantified and analyzed by one sample t-test. Data are shown as the mean ± SD. *P<0.05, **P<0.01 and ***P<0.001, n=3. (F) Left panel: The subcellular fraction was isolated using nuclear and cytoplasmic protein extraction kit according to manufacturer's instructions. The SMAD3 level was detected by western blotting, α-tubulin and lamin A/C were used as cytosolic and nuclear internal controls. Right panel: IF analysis of SMAD3 in AGS cells treated with or without rabeprazole for 1 h. Scale bar, 100 μm. SMAD3, SMAD family member 3; IF, immunofluorescence; phospho, phosphorylated.

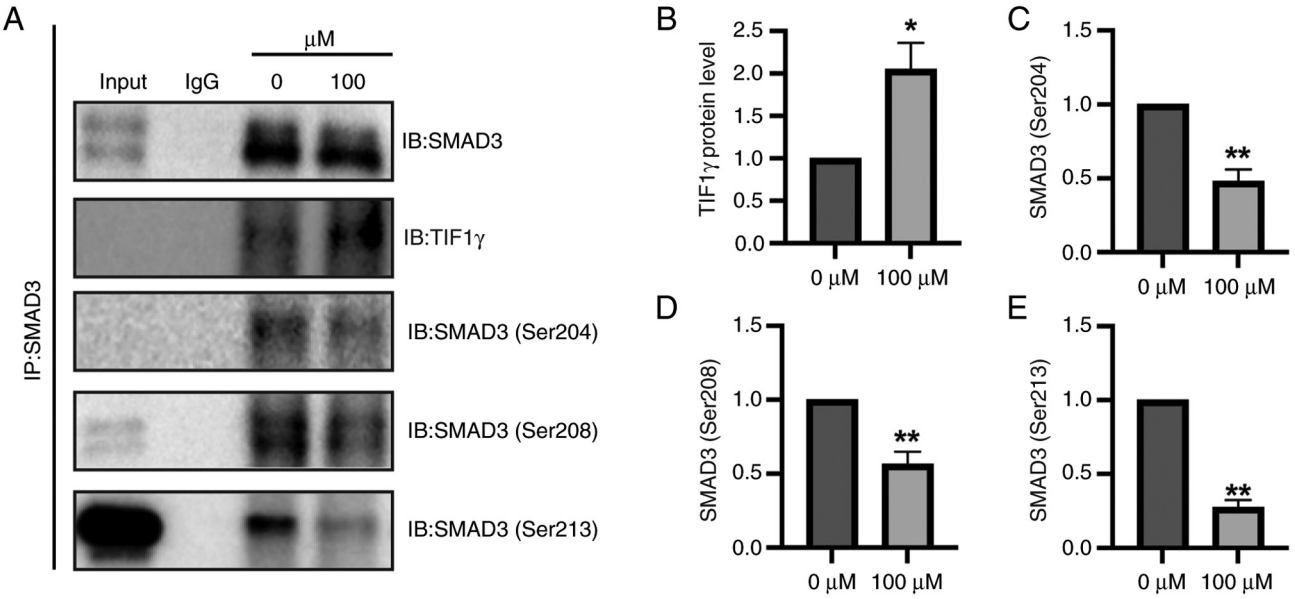

Figure 4. Rabeprazole modulates the TIF1γ/SMAD3 complex. (A) Following overnight serum starvation, AGS cells were treated with or without rabeprazole for 1 h, and an IP experiment with anti-SMAD3 or IgG was performed. Immunoblotting was employed to analyze the indicated protein expression levels. (B-E) Band intensities were quantified and the differences were analyzed. Data are shown as the mean ± SD and determined using one sample t-test; *P<0.05 and **P<0.01; n=3. TIF1γ, transcriptional intermediary factor 1γ; SMAD3, SMAD family member 3; IP, immunoprecipitation.

assays further revealed that rabeprazole treatment led to a significantly enhanced SMAD3/TIF1γ complex, which in turn further inhibited SMAD3 linker phosphorylation, including Ser204, Ser208 and Ser213 (Fig. 4A-E), consistent with our other research work showing that overexpression of TIF1γ led to inhibition of SMAD3 phosphorylation (Li *et al* unpublished data). These results indicated that rabeprazole treatment led to an antifibrotic TIF1γ/SMAD3 complex.

Discussion

Fibrosis is a common pathological change in various diseases, including chronic hepatitis B-related liver diseases (30) and gastrointestinal-related diseases (31). Previous studies demonstrated that rabeprazole has various biological functions (9,29,32,33), however, the present study further revealed a novel mechanism of rabeprazole in fibrosis. The present study found that rabeprazole exerted an inhibitory effect on fibrosis, which was attributed to enhanced TIF1γ expression, while enhanced TIF1γ expression could inhibit SMAD3 linker phosphorylation. Further analysis showed that TIF1γ interacted with SMAD3, leading to suppression of SMAD3 signaling characterized by decreased phosphorylation of SMAD3 linker at Ser213, Ser204 and Ser208, and rabeprazole treatment enhanced this interaction between TIF1γ and SMAD3 to aggravate SMAD3 linker phosphorylation inhibition to alleviate fibrosis. This finding not only enriched the knowledge on the biological function of rabeprazole, but also the provided a possible therapeutic strategy for fibrosis.

Rabeprazole, a well-known PPI, was reported to induce M2-type adipose tissue macrophages, alleviating chronic inflammation (18), and to improve the survival rate and ameliorate pathological damage in *Clostridium perfringens* or perfringolysin O (PFO)-treated *Galleria mellonella* (34). Moreover, rabeprazole was shown to have anti-*Trypanosoma cruzi* activity by targeting cellular triosephosphate isomerase (35). Rabeprazole has been demonstrated to destroy gastric epithelial barrier function *in vivo* and *in vitro* (20,36), while exhibiting nephroprotective effects through inhibition of organic cation transporter 2 (37) as well as promoting vascular impairment through hypoxia-inducible factor 1-α (38). The present study further investigated the antifibrotic function of rabeprazole. In previous studies, rabeprazole was demonstrated to induce enhanced TIF1γ expression, leading to suppression of TGFβ signaling. Notably, phosphorylation of TIF1γ at Tyr-524, Tyr-610, and Tyr-1048 was found to destroy the complex between TIF1γ and SMAD3, which could enhance TGFβ signaling (17,39). Therefore, further investigation was required to reveal the mechanism through which rabeprazole regulated TIF1γ expression. However, the influence of rabeprazole on TIF1γ phosphorylation remains unclear and will require further investigations. In addition, the present study lacked *in vivo* experiments confirming the possible role of rabeprazole in fibrosis. Furthermore, phosphorylation of SMAD3, at both the linker domain and C-terminus, is a critical event for the initiation of fibrosis or EMT (40). Phosphorylation of SMAD3 at Ser204, Ser208, and Ser213 was observed to be significantly reduced in response to rabeprazole stimulation, and this phenomenon was attributed to the formation of an enhanced complex between TIF1γ and SMAD3 caused by rabeprazole. However, the specific domain and phosphorylation status of TIF1γ that facilitate its interaction with SMAD3, particularly under rabeprazole treatment, remain unclear. In addition, considering that the disease and tumor microenvironment are enriched with diverse inflammatory and immune cells, including macrophages and fibroblasts, our future work will employ progressively complex *in vitro* systems, ranging from spheroid and organoid-based co-cultures to air-liquid interface organoids and microfluidic organoid-on-a-chip platforms. These models will be used to investigate whether rabeprazole plays a role in remodeling the cellular microenvironment (41,42).

In summary, the present study revealed a novel antifibrotic role of rabeprazole *in vitro*, mediated through the formation of a TIF1γ-SMAD3 complex. These findings offer novel insights into the biological functions of rabeprazole and suggest its potential as an alternative therapeutic strategy for fibrosis-related diseases.

Acknowledgements

Not applicable.

Funding

The present study was supported by the Science and Technology Project in the Field of Social Development of Zhuhai (grant. no. 2220004000296).

Availability of data and materials

The data generated in the present study are included in the figures and/or tables of this article.

Authors' contributions

LL, XT and JC designed the experiments. LL, ZL and LF performed the experiments and data collection. LL, YC and XT analyzed the data and generated the figures. LL, XT and JC drafted the manuscript and revised the manuscript. LL and XT confirm the authenticity of all the raw data. All authors read and approved the final version of the manuscript.

Ethics approval and consent to participate

Not applicable.

Patient consent for publication

Not applicable.

Competing interests

The authors declare that they have no competing interests.

References

1. Luo L, Zhang W, You S, Cui X, Tu H, Yi Q, Wu J and Liu O: The role of epithelial cells in fibrosis: Mechanisms and treatment. Pharmacol Res 202: 107144, 2024.
2. Hanahan D and Weinberg RA: Hallmarks of cancer: The next generation. Cell 144: 646-674, 2011.
3. Thiery JP, Acloque H, Huang RY and Nieto MA: Epithelial-mesenchymal transitions in development and disease. Cell 139: 871-890, 2009.
4. Kalluri R and Weinberg RA: The basics of epithelial-mesenchymal transition. J Clin Invest 119: 1420-1428, 2009.
5. Li Y, Ren BX, Li HM, Lu T, Fu R and Wu ZQ: Omeprazole suppresses aggressive cancer growth and metastasis in mice through promoting Snail degradation. Acta Pharmacol Sin 43: 1816-1828, 2022.
6. Zhang B, Ling T, Zhaxi P, Cao Y, Qian L, Zhao D, Kang W, Zhang W, Wang L, Xu G and Zou X: Proton pump inhibitor pantoprazole inhibits gastric cancer metastasis via suppression of telomerase reverse transcriptase gene expression. Cancer Lett 452: 23-30, 2019.
7. Feng S, Zheng Z, Feng L, Yang L, Chen Z, Lin Y, Gao Y and Chen Y: Proton pump inhibitor pantoprazole inhibits the proliferation, self-renewal and chemoresistance of gastric cancer stem cells via the EMT/β-catenin pathways. Oncol Rep 36: 3207-3214, 2016.
8. Zhang B, Yang Y, Shi X, Liao W, Chen M, Cheng AS, Yan H, Fang C, Zhang S, Xu G, *et al*: Proton pump inhibitor pantoprazole abrogates adriamycin-resistant gastric cancer cell invasiveness via suppression of Akt/GSK-β/β-catenin signaling and Epithelial-mesenchymal transition. Cancer Lett 356: 704-712, 2015.
9. Babu D, Mudiraj A, Yadav N, Y B V K C, Panigrahi M and Prakash Babu P: Rabeprazole has efficacy per se and reduces resistance to temozolomide in glioma via EMT inhibition. Cell Oncol (Dordr) 44: 889-905, 2021.
10. Dooley S, Said HM, Gressner AM, Floege J, En-Nia A and Mertens PR: Y-box protein-1 is the crucial mediator of antifibrotic interferon-gamma effects. J Biol Chem 281: 1784-1795, 2006.
11. Higashi K, Inagaki Y, Fujimori K, Nakao A, Kaneko H and Nakatsuka I: Interferon-gamma interferes with transforming growth factor-beta signaling through direct interaction of YB-1 with Smad3. J Biol Chem 278: 43470-43479, 2003.
12. Lee EJ, Hwang I, Lee JY, Park JN, Kim KC, Kim I, Moon D, Park H, Lee SY, Kim HS, *et al*: Hepatic stellate cell-specific knockout of transcriptional intermediary factor 1γ aggravates liver fibrosis. J Exp Med 217: e20190402, 2020.
13. Ikeuchi Y, Dadakhujaev S, Chandhoke AS, Huynh MA, Oldenborg A, Ikeuchi M, Deng L, Bennett EJ, Harper JW, Bonni A and Bonni S: TIF1γ protein regulates epithelial-mesenchymal transition by operating as a small ubiquitin-like modifier (SUMO) E3 ligase for the transcriptional regulator SnoN1. J Biol Chem 289: 25067-25078, 2014.
14. Su Z, Sun Z, Wang Z, Wang S, Wang Y, Jin E, Li C, Zhao J, Liu Z, Zhou Z, *et al*: TIF1γ inhibits lung adenocarcinoma EMT and metastasis by interacting with the TAF15/TBP complex. Cell Rep 41: 111513, 2022.
15. Matsuzaki K: Smad3 phosphoisoform-mediated signaling during sporadic human colorectal carcinogenesis. Histol Histopathol 21: 645-662, 2006.
16. Ooshima A, Park J and Kim SJ: Phosphorylation status at Smad3 linker region modulates transforming growth factor-β-induced Epithelial-mesenchymal transition and cancer progression. Cancer Sci 110: 481-488, 2019.
17. He W, Dorn DC, Erdjument-Bromage H, Tempst P, Moore MA and Massague J: Hematopoiesis controlled by distinct TIF1gamma and Smad4 branches of the TGFbeta pathway. Cell 125: 929-941, 2006.
18. Li Y, Hao J, Kong X, Yuan W, Shen Y, Hui Z and Lu X: Rabeprazole mitigates obesity-induced chronic inflammation and insulin resistance associated with increased M2-type macrophage polarization. Biochim Biophys Acta Mol Basis Dis 1870: 167142, 2024.
19. Chen SQ, Hu BF, Yang YR, He Y, Yue L, Guo D, Wu TN, Feng XW, Li Q, Zhang W and Wen JG: The protective effect of rabeprazole on cisplatin-induced apoptosis and necroptosis of renal proximal tubular cells. Biochem Biophys Res Commun 612: 91-98, 2022.
20. Yang F, Li L, Zhou Y, Pan W, Liang X, Huang L, Huang J, Cheng Y, Geng L, Xu W and Gong S: Rabeprazole destroyed gastric epithelial barrier function through FOXF1/STAT3-mediated ZO-1 expression. Clin Exp Pharmacol Physiol 50: 516-526, 2023.
21. Son M, Park IS, Kim S, Ma HW, Kim JH, Kim TI, Kim WH, Han J, Kim SW and Cheon JH: Novel Potassium-competitive acid blocker, tegoprazan, protects against colitis by improving gut barrier function. Front Immunol 13: 870817, 2022.
22. Zhou Y, Chen S, Yang F, Zhang Y, Xiong L, Zhao J, Huang L, Chen P, Ren L, Li H, *et al*: Rabeprazole suppresses cell proliferation in gastric epithelial cells by targeting STAT3-mediated glycolysis. Biochem Pharmacol 188: 114525, 2021.
23. Niu R, Lan J, Liang D, Xiang L, Wu J, Zhang X, Li Z, Chen H, Geng L, Xu W, *et al*: GZMA suppressed GPX4-mediated ferroptosis to improve intestinal mucosal barrier function in inflammatory bowel disease. Cell Commun Signal 22: 474, 2024.
24. Li P, Wu Y, Deng Z, Samad A, Xi Y, Song J, Zhang Y, Li J, Zhou YA, Xiong Q and Wu C: Two novel SH3TC2 mutations predispose to Charcot-Marie-Tooth disease type 4C by mistargeting away from TFRC. Cell Signal 130: 111669, 2025.
25. Hesling C, Fattet L, Teyre G, Jury D, Gonzalo P, Lopez J, Vanbelle C, Morel AP, Gillet G, Mikaelian I and Rimokh R: Antagonistic regulation of EMT by TIF1γ and Smad4 in mammary epithelial cells. EMBO Rep 12: 665-672, 2011.

26. Qi G, Lu G, Yu J, Zhao Y, Wang C, Zhang H and Xia Q: Up-regulation of TIF1γ by valproic acid inhibits the epithelial mesenchymal transition in prostate carcinoma through TGF-β/Smad signaling pathway. Eur J Pharmacol 860: 172551, 2019.
27. Yin X, Xu C, Zheng X, Yuan H, Liu M, Qiu Y and Chen J: SnoN suppresses TGF-β-induced epithelial-mesenchymal transition and invasion of bladder cancer in a TIF1γ-dependent manner. Oncol Rep 36: 1535-1541, 2016.
28. Sun YM, Wu Y, Li GX, Liang HF, Yong TY, Li Z, Zhang B, Chen XP, Jin GN and Ding ZY: TGF-β downstream of Smad3 and MAPK signaling antagonistically regulate the viability and partial epithelial-mesenchymal transition of liver progenitor cells. Aging (Albany NY) 16: 6588-6612, 2024.
29. Zheng M, Li H, Sun L, Cui S, Zhang W, Gao Y and Gao R: Calcipotriol abrogates TGF-β1/pSmad3-mediated collagen 1 synthesis in pancreatic stellate cells by downregulating RUNX1. Toxicol Appl Pharmacol 491: 117078, 2024.
30. Xiao J, Liu H, Yao J, Yang S, Shen F, Bu K, Wang Z, Liu F, Xia N and Yuan Q: The characterization of serum proteomics and metabolomics across the cancer trajectory in chronic hepatitis B-related liver diseases. View: 5, 2024.
31. Ito T and Kayama H: Roles of fibroblasts in the pathogenesis of inflammatory bowel diseases and IBD-associated fibrosis. Int Immunol 37: 377-392, 2025.
32. Xie J, Liang X, Xie F, Huang C, Lin Z, Xie S, Yang F, Zheng F, Geng L, Xu W, *et al*: Rabeprazole suppressed gastric intestinal metaplasia through activation of GPX4-mediated ferroptosis. Front Pharmacol 15: 1409001, 2024.
33. Gu M, Zhang Y, Zhou X, Ma H, Yao H and Ji F: Rabeprazole exhibits antiproliferative effects on human gastric cancer cell lines. Oncol Lett 8: 1739-1744, 2014.
34. Wang G, Liu Y, Deng L, Liu H, Deng X, Li Q, Feng H, Guo Z and Qiu J: Repurposing rabeprazole sodium as an anti-*Clostridium perfringens* drug by inhibiting perfringolysin O. J Appl Microbiol 134: 2023.
35. Garcia-Torres I, De la Mora-De la Mora I, Lopez-Velazquez G, Cabrera N, Flores-López LA, Becker I, Herrera-López J, Hernández R, Pérez-Montfort R and Enríquez-Flores S: Repurposing of rabeprazole as an anti-*Trypanosoma cruzi* drug that targets cellular triosephosphate isomerase. J Enzyme Inhib Med Chem 38: 2231169, 2023.
36. Takashima S, Tanaka F, Kawaguchi Y, Usui Y, Fujimoto K, Nadatani Y, Otani K, Hosomi S, Nagami Y, Kamata N, *et al*: Proton pump inhibitors enhance intestinal permeability via dysbiosis of gut microbiota under stressed conditions in mice. Neurogastroenterol Motil 32: e13841, 2020.
37. Sharaf G, E ME and El-Sayed EK: Augmented nephroprotective effect of liraglutide and rabeprazole via inhibition of OCT2 transporter in cisplatin-induced nephrotoxicity in rats. Life Sci 321: 121609, 2023.
38. Evans CE, Peng Y, Zhu MM, Dai Z, Zhang X and Zhao YY: Rabeprazole promotes vascular repair and resolution of Sepsis-induced inflammatory lung injury through HIF-1α. Cells 11: 1425, 2022.
39. Yuki R, Tatewaki T, Yamaguchi N, Aoyama K, Honda T, Kubota S, Morii M, Manabe I, Kuga T, Tomonaga T and Yamaguchi N: Desuppression of TGF-β signaling via nuclear c-Abl-mediated phosphorylation of TIF1γ/TRIM33 at Tyr-524, -610, and -1048. Oncogene 38: 637-655, 2019.
40. Matsuzaki K: Smad phospho-isoforms direct context-dependent TGF-β signaling. Cytokine Growth Factor Rev 24: 385-399, 2013.
41. Zhou PZ, Gao L, Wang LW, Zhang YF, Song WL and Hao YX: Clinical observation of magnesium aluminum carbonate combined with rabeprazole-based triple therapy in the treatment of helicobacter pylori-positive gastric ulcer associated with hemorrhage. Pak J Med Sci 38: 1271-1277, 2022.
42. Yuan K, Du X, Dong L, Pan J and Xue W: Modelling the tumor microenvironment in vitro in prostate cancer: Current and future perspectives. VIEW: 5: 20240074, 2024.